Oriented growth during recrystallization revisited in three dimensions

Fan, Guohua; Zhang, Yubin; Driver, J. H.; Juul Jensen, Dorte

Published in:
Scripta Materialia

Link to article, DOI:
10.1016/j.scriptamat.2013.09.031

Publication date:
2014

Document Version
Publisher's PDF, also known as Version of record

Available online at www.sciencedirect.com

ScienceDirect

Scripta Materialia 72–73 (2014) 9–12

Scripta MATERIALIA

www.elsevier.com/locate/scriptamat

Oriented growth during recrystallization revisited in three dimensions☆

G.H. Fan,[a,b] Y.B. Zhang,[b] J.H. Driver[c] and D. Juul Jensen[b,*]

[a]*School of Materials Science and Engineering, Harbin Institute of Technology, Harbin 150001, People's Republic of China*
[b]*Danish–Chinese Center for Nanometals, Section for Materials Science and Advanced Characterization, Department of Wind Energy, Technical University of Denmark, Risø Campus, DK-4000 Roskilde, Denmark*
[c]*Ecole des Mines de Saint Etienne, Centre SMS, 158 Cours Fauriel, 42023 Saint Etienne Cedex 2, France*

Received 17 September 2013; revised 27 September 2013; accepted 29 September 2013
Available online 8 October 2013

The two surfaces of a 40% cold-rolled tricrystal of aluminium were scratched to stimulate recrystallization nucleation. Serial sectioning combined with electron backscatter diffraction was used to characterize the nuclei in three dimensions. It was found that the largest nuclei have a 40°⟨1 1 1⟩ relationship to the matrix, but there are also many nuclei of this orientation relationship which do not grow to large sizes. It is shown that local variations in the deformation microstructure determine where preferential growth occurs.

Keywords: Tricrystal; Aluminium; Recrystallization; Electron backscatter diffraction (EBSD); Nucleation

Growth during recrystallization is determined by the orientation of the available nuclei (i.e. the nuclei that have formed) and by the deformation microstructure in which they grow. Barrett [1] was the first to suggest that grain boundary mobility depends on the misorientation across the boundary. The experimental verification of this idea was provided by the classical Beck experiment [2], in which growth of artificially stimulated nuclei into a lightly deformed single crystal was studied. Later several groups performed experiments of this type and for face-centred-cubic (fcc) metals it was generally found that nuclei with a misorientation of ~40° around a common ⟨1 1 1⟩ axis grew the fastest [2–6]. Also analysis of texture change during recrystallization tends to support a preferential 40°⟨1 1 1⟩ growth [7]. The magnitude of the preferential growth advantage was observed to depend on materials and process parameters such as purity and solute content [8–10] as well as annealing temperature [11,12]. The actual grain boundary plane was also found to be of importance, and Kohara et al. [13] and Parthasarathi and Beck [14] observed that tilt boundaries move faster than twist boundaries in fcc metals.

The aim of the present work is to revisit this classical work on preferential growth during recrystallization. The novel aspect of this work relates to two factors:

1. A large tricrystal is used instead of a single crystal. This allows for an investigation of the importance of the deformed microstructure morphology, including stored energy variations which exist between the three different crystals, on the growth of artificially stimulated nuclei under otherwise identical conditions in one experiment.
2. The investigation is done in three dimensions. By having the full three-dimensional (3-D) picture, possible pitfalls from the previous more limited two-dimensional (2-D) investigations are avoided. Compared to the texture investigations the present work benefits from knowing the 3-D shapes of the nuclei, and the direct relationship to the local deformed matrix.

It is found that both these factors are important for interpreting the preferential growth results.

A high-purity (99.99%) tricrystal of aluminium with the growth direction triple line along the crystallographic ⟨1 1 0⟩ axes was prepared by directional solidification. A sketch of the sample is shown in Figure 1a. The three crystals are labelled as A, B and C, and their orientations

* Corresponding author. Tel.: +45 46775701; fax: +45 46775758; e-mail: doje@dtu.dk

1359-6462/$ - see front matter
http://dx.doi.org/10.1016/j.scriptamat.2013.09.031

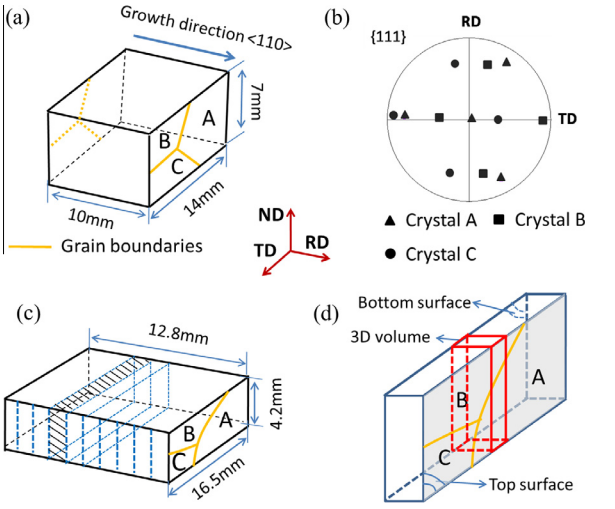

Figure 1. Sketches of the aluminium tricrystal sample: (a) the geometry of the tricrystal with the growth direction along the crystallographic ⟨1 1 0⟩ axes and (b) a {1 1 1} pole figure showing the orientations of the three crystals; (c) schematic drawing of rolled sample which was divided into ten slices; (d) the geometry of slice No. 4 as highlighted in (c). The "top surface" is indicated in grey and the sketch shows the details of the serial section volume (red box).

are ∼(1 1 –1)[1 0 1], ∼(1 3 –1)[1 0 1] and ∼(−3–1 1)[0 1 1], respectively (Fig. 1b), which correspond to "medium hard", "soft" and "soft" orientations according to Taylor factor calculations, (∼3.7 for A and ∼2.4 for B and C).

The tricrystal was cold rolled to 40% reduction with the triple line parallel to the rolling direction (RD). Rolling was conducted applying intermediate passes under conditions of $l/h \sim 2$, where l is the length of contact between the rolls and the specimen and h is the mean sample thickness. After rolling, the sample was sectioned perpendicular to the RD into ten 1 mm thick slices as shown in Figure 1c. The surfaces on the normal direction–transverse direction (ND–TD) planes of slice No. 4, i.e. top and bottom surfaces in Figure 1d, were rubbed with emery paper as randomly as possible, in order to stimulate artificial preferential nucleation. Slice No. 4 was then annealed at 300 °C for 20 min in an air furnace to initiate recrystallization. The top surface of slice No. 4 (see Fig. 1d) was electropolished, while the bottom surface was preserved as the originally scratched surface.

A sample from slice No. 4 near the triple junction (red box in Fig. 1d) was serial sectioned along the TD. In each section an area of 3 mm × 0.8 mm was characterized by electron backscatter diffraction (EBSD) with a step size of 2 μm using a Zeiss Supra 35 thermal field emission gun scanning electron microscope. A detailed description of the serial sectioning and alignment procedure can be found in the Supplementary material and in Refs. [15,16].

The partially recrystallized microstructure seen within a ND–RD section is shown in Figure 2. Focusing on the non-recrystallized microstructure, it is evident that crystal A is significantly subdivided, consisting of some narrow deformation bands with large misorientations (maximum misorientation angle ∼45°) near the grain boundary (between crystal A and B), a large transition band and wide deformation bands as marked in Figure 2 (see also Figs. S3 and S4 in the Supplementary material). The crystal B is far less subdivided, consisting of mainly diffuse transition bands. These differences in microstructures of the crystals will be described in more detail in Ref. [17].

As seen in Figure 2, the recrystallizing nuclei/grains are found mainly in crystal A, at the scratched surfaces and within the deformed matrix, in particular at the narrow deformation bands and transition bands. Only seven very small nuclei/grains are found in crystal B at the bottom scratched surface (see Figs. 2 and S3). These seven nuclei/grains have no apparent preferential orientation relationship to the matrix.

For crystal A we shall in this paper only analyse the nuclei stimulated by scratches which can best be seen on the bottom surface, which was not electropolished, and thus also the smallest nuclei are visible. Nuclei formed within the deformed matrix of crystal A will be investigated in Ref. [17]. For simplicity, in the following the

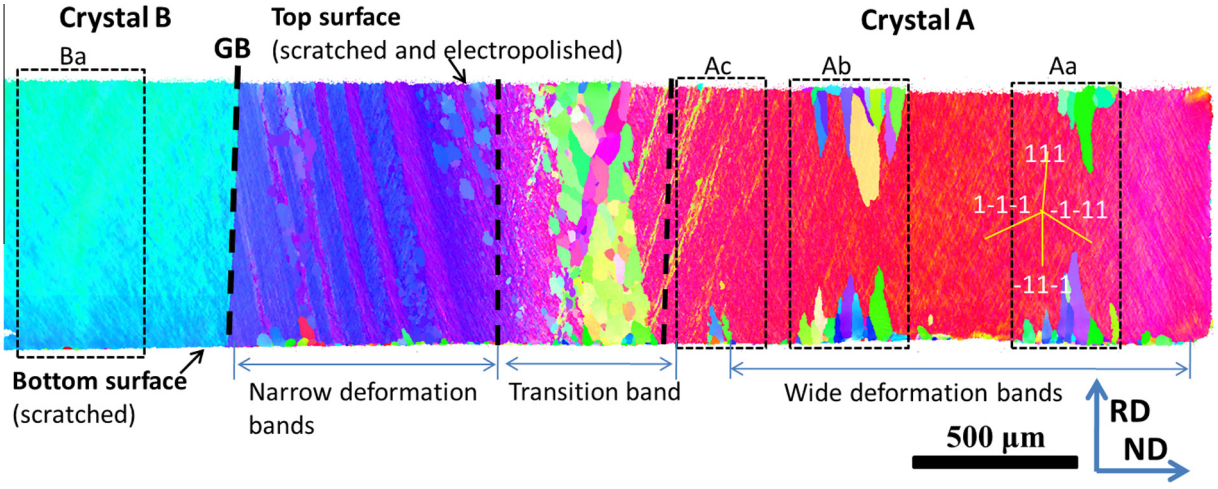

Figure 2. (a) EBSD map showing the partially recrystallized microstructure on the ND–RD section of the first sectioned layer. The colours represent the crystallographic direction of the TD (see Fig. S2).

term "nuclei/grains" refers to the nuclei/grains in crystal A stimulated by the scratches.

In total 287 nuclei/grains were found in the investigated 3-D volume. A large fraction of the nuclei/grains share {1 1 1} poles with the deformed microstructure, while the rest have relatively random orientations (see Fig. S3). The sizes of the nuclei/grains vary significantly from location to location, and the largest nuclei are found at the edges of the two wide deformation bands in the regions marked Aa and Ab (see Fig. 2).

The full 3-D shape of the nuclei/grains has been reconstructed. An example of nuclei/grains at the bottom surface in region Aa (see Fig. 2) is shown in Figure 3. It is evident that the large grains typically are elongated along two directions inclined about 20–25° and 35–40° to the TD, which are approximately parallel to the (1 1 1) and (−1 1 −1) planes of the deformed crystal A. The smaller grains are generally fairly equiaxed. Figure 3 also shows that the grain sizes of any nucleus/grain seen in the 2-D sections vary a lot along the TD.

The volumes of nuclei/grains measured based on the 3-D data are shown as a function of misorientation to the local deformed microstructure in Figure 4a and c. For comparison, the areas of nuclei/grains seen in the second sectioned layer are shown also as a function of misorientation in Figure 4b and d. The misorientations in Figure 4 are calculated between the orientation of each nucleus/grain and its nearest neighbouring orientation in the deformed matrix at the peak position of the nucleus/grain (furthest away from the scratched surface) along the RD in the full 3-D volume (For the 2-D measurements only in the second layer). It is evident that a sharp peak at ~40° is observed in three dimensions, whereas a broad, almost double, peak is observed in two dimensions. A similar double peak is observed and discussed in Ref. [12]. The following analysis is based on the 3-D dataset.

Figure 4a shows that the sizes of the nuclei/grains vary over a wide range. Whereas most nuclei/grains are relatively small and have a broad range of misorientations to the deformed matrix, a small fraction (about 49, ~10%) of the nuclei/grains is quite large (nuclei volume $\geqslant 30 \times 10^4$ μm^3). It is generally assumed that large grains have benefited from a growth preference of the 40°⟨1 1 1⟩ boundaries (Σ7 boundaries) [2–7,12]. If the Brandon criteria are used [18], it is, however, found that

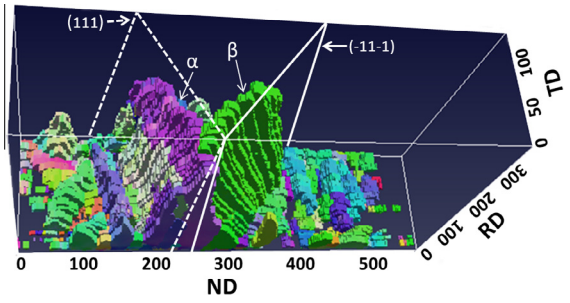

Figure 3. 3-D reconstruction of the nuclei/grains at the bottom sample surface within region Aa in Figure 2. α and β are used to mark two large grains. The positions of (−1 1 −1) and (1 1 1) planes of the deformed matrix are approximately marked by solid and dashed lines, respectively.

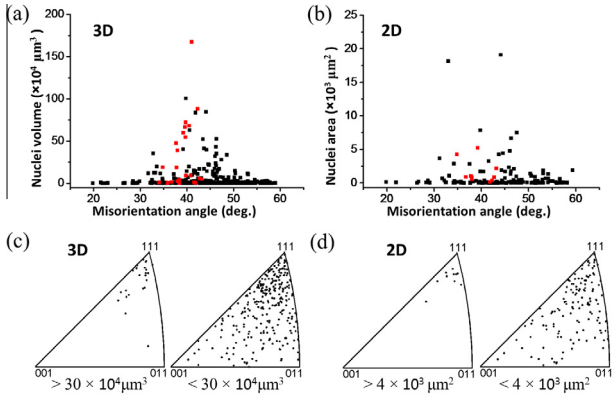

Figure 4. Size vs. misorientation angle distribution of scratch-stimulated recrystallizing nuclei/grains in (a) three dimensions and (b) two dimensions. Red dots represent nuclei with Σ7 boundaries to the surrounding matrix and black dots all other misorientations. (c, d) Distributions of rotation axes of scratch-stimulated nuclei/grains with different size.

only a relatively small fraction of boundaries between nuclei/grains and deformed matrix are Σ7 boundaries. These are highlighted in red in Figure 4a and b.

It is important to notice that the largest nucleus/grain (170×10^4 μm^3) does indeed have a Σ7 misorientation, and the present result thus agrees well with the classic Beck experiment, which also focused on the largest nuclei/grains [2]. Considering that only one orientation from the deformed matrix was chosen for the calculation of misorientation and that a large orientation spread exists in the deformed microstructure, several of the other large nuclei/grains may also have experienced Σ7 relationships earlier during their growth. The orientation spread in the deformed microstructure is wide and varies from region to region. For example, in region Aa (see Fig. 2) the spread is ~20° and as this region is of particular interest (to be discussed later), all boundaries having misorientation of 40 ± 10° with rotation axes deviating less than 20° from ⟨1 1 1⟩ may be considered to be the 40°⟨1 1 1⟩-type. With this definition it is observed that all large ($\geqslant 30 \times 10^4$ μm^3) nuclei/grains have the 40°⟨1 1 1⟩ misorientation relationship, but there are also 89 nuclei/grains with volumes less than 30×10^4 μm^3 which have the 40°⟨1 1 1⟩ misorientation. The growth of some of these small 40°⟨1 1 1⟩ nuclei/grains may be stopped by impingement with other nuclei/grains, but small non-impinged 40°⟨1 1 1⟩ nuclei/grains are indeed observed.

In total 138 out of the 287 nuclei/grains have a 40°⟨1 1 1⟩-type relationship to the matrix. Detailed analysis of these nuclei/grains shows that all eight possible 40°⟨1 1 1⟩ relationships are found (see Table 1). In Table 1 nuclei/grains are separated according to the common {1 1 1} planes between each nucleus/grain and its neighbouring matrix as well as rotation "+" and "−" 40° ± 10° around the normal of the common plane. Nuclei/grains not belonging to the 40°⟨1 1 1⟩ groups are referred as "random".

It is evident that a relatively large number of nuclei/grains (~40%) share (1 1 1) and (−1 1 −1) planes with the deformed matrix and the average grain size of these nuclei/grains are much larger than those of random ori-

Table 1. Number and average volume of nuclei/grains with misorientations of 40 ± 10° with rotation axis within 20° of ⟨1 1 1⟩ and as well as nuclei/grains with random misorientations.

Rotation axes	Misorientation to surrounding deformed matrix								
	~[−1 1 −1]		~[1 1 1]		~[1 −1 −1]		~[−1 −1 1]		Random
	+	−	+	−	+	−	+	−	
No. of nuclei	28	18	42	26	6	7	4	7	149
Average volume ($\times 10^4$ μm^3)	23.4 ± 37.0	21.1 ± 26.5	14.8 ± 22.7	11.6 ± 15.4	6.3 ± 11.1	6.1 ± 14.8	1.0 ± 1.2	2.6 ± 4.7	1.4 ± 2.4

entations (see Table 1). Example of these nuclei/grains can be seen in Figure 3 as marked by α and β. It is clear that the growth directions of nuclei/grains in these two groups are parallel more or less to the (1 1 1) and (−1 1 −1) planes, respectively. In other words, the fast migrating boundaries are tilt boundaries and the lenticular shape of nuclei/grains develops by the fast migration of 40°⟨1 1 1⟩ tilt boundaries, which agrees well with the classic observations [13,14].

An important observation in the present work is that the largest nuclei/grains are not observed at random positions on the scratched surfaces, as would have been expected if the misorientation was the only important parameter. Figure 2 clearly reveals that the large nuclei/grains are clustered in certain regions (regions Aa and Ab). These regions are observed to have relatively high local stored energies which clearly contribute to fast nucleation and growth of nuclei/grains formed in these regions (see Fig. S4). A further observation is that the dislocation structure within the fast growing regions Aa and Ab consists of dislocation boundaries aligned more or less parallel to the (1 1 1) and (−1 1 −1) planes (see Figs. 2 and S3). This agrees with suggestions based on previous 2-D observations [5,19]. However, the present 3-D observations additionally reveal that if the dominating dislocation boundaries are less favourably aligned or the deformation structure is complex with many dominating dislocation boundaries in various directions, the scratch stimulated nuclei/grains – even the 40°⟨1 1 1⟩ misoriented ones – grow only slowly. This important observation can only be verified with the 3-D data set.

In summary, the growth of artificially stimulated nuclei in a 40% cold rolled aluminium tricrystal was studied in three dimensions by serial sectioning and EBSD characterizations. It was found that if only a 2-D section is characterized, a complex relationship is observed between the nuclei/grains sizes and their misorientations to the deformed matrix; for example, the 2-D distribution is observed to have a double peak with grains rotated 33° and 44° being the largest. When the full 3-D data for the same grains are analysed, it becomes apparent that the truly largest grain has a 40°⟨1 1 1⟩(Σ7) relationship to the matrix. A further important result of the present work is that the misorientation is not the only parameter which determines the growth rates of the nuclei/grains. The morphology of the deformed microstructure and local variations in stored energy are also of utmost importance. It is suggested that early nucleation occurs in local regions with high stored energy and that preferential growth occurs in local regions, where the local stored energy is high and the dislocation boundaries are favourably arranged in the deformed crystal.

The authors gratefully acknowledge the support from the Danish National Research Foundation (Grant No. DNRF86-5) and the National Natural Science Foundation of China (Grant No. 51261130091) to the Danish–Chinese Center for Nanometals, within which this work has been performed.

Supplementary data associated with this article can be found, in the online version, at http://dx.doi.org/10.1016/j.scriptamat.2013.09.031.

[1] C.S. Barrett, Trans. AIME 137 (1940) 128–149.
[2] P.A. Beck, P.R. Sperry, H. Hu, J. Appl. Phys. 21 (1950) 420–425.
[3] B. Liebmann, K. Lücke, G. Masing, Z. Metallkd. 47 (1956) 57–63.
[4] S. Kohara, M.N. Parthasarathi, P.A. Beck, Trans. Metall. Soc. AIME 212 (1958) 875.
[5] H. Yoshida, B. Liebmann, K. Lücke, Acta Metall. 7 (1959) 51–56.
[6] G. Ibe, K. Lücke, in: H. Margolin (Ed.), Recrystallization, Grain Growth and Texture, ASM, Metals Park, OH, 1966, pp. 434–447.
[7] O. Engler, Mater. Sci. Technol. 12 (1996) 859–872.
[8] K.T. Aust, J.W. Rutter, Trans. Metall. Soc. AIME 218 (1960) 50.
[9] P. Gordon, R.A. Vandermeer, in: H. Margolin (Ed.), Recrystallization, Grain Growth and Texture, ASM, Metals Park, OH, 1966, pp. 205–266.
[10] M.L. Taheri, A.D. Rollett, H. Weiland, Mater. Sci. Forum 467–470 (2004) 997–1002.
[11] K.T. Aust, J.W. Rutter, Trans. Metall. Soc. AIME 224 (1962) 111.
[12] M.L. Taheri, D. Molodov, G. Gottstein, A.D. Rollett, Z. Metallkd. 96 (2005) 1166–1170.
[13] S. Kohara, M.N. Parthasarathi, P.A. Beck, J. Appl. Phys. 29 (1958) 1125–1126.
[14] M.N. Parthasarathi, P.A. Beck, Trans. Metall. Soc. AIME 221 (1961) 831–836.
[15] F.X. Lin, A. Godfrey, D. Juul Jensen, G. Winther, Mater. Charact. 61 (2010) 1203–1210.
[16] Y.H. Zhang, D. Juul Jensen, Y.B. Zhang, F.X. Lin, Z.Q. Zhang, Q. Liu, Scripta Mater. 67 (2012) 320–323.
[17] G.H. Fan, R. Quey, Y.B. Zhang, J. H. Driver, D. Juul Jensen, in preparation.
[18] D.G. Brandon, Acta Metall. Mater. 14 (1966) 1479–1484.
[19] H. Paul, J.H. Driver, C. Maurice, A. Piatkowski, Acta Mater. 55 (2007) 833–847.